Cancer Letters 508 (2021) 18–29

Contents lists available at ScienceDirect

Cancer Letters

journal homepage: www.elsevier.com/locate/canlet

Pharmacological inhibition of 17β-hydroxysteroid dehydrogenase impairs human endometrial cancer growth in an orthotopic xenograft mouse model

Sofia Xanthoulea [a,b,*,2], Gonda F.J. Konings [a,b,2], Niina Saarinen [c,d], Bert Delvoux [a,b], Loes F. S. Kooreman [a,e], Pasi Koskimies [c], Merja R. Häkkinen [f], Seppo Auriola [f], Elisabetta D'Avanzo [a,b], Youssef Walid [a,b], Frank Verhaegen [a], Natasja G. Lieuwes [a,g], Florian Caiment [a,h], Roy Kruitwagen [a,b], ENITEC[1], Andrea Romano [a,b]

[a] *GROW – School for Oncology & Developmental Biology, Maastricht University, the Netherlands*
[b] *Department of Obstetrics and Gynaecology, Maastricht University Medical Centre, the Netherlands*
[c] *Forendo Pharma Ltd., Turku, Finland*
[d] *Institute of Biomedicine, Research Centre for Integrative Physiology and Pharmacology and Turku Center for Disease Modeling (TCDM), University of Turku, Finland*
[e] *Department of Pathology, Maastricht University Medical Centre, the Netherlands*
[f] *School of Pharmacy, University of Eastern Finland, Kuopio, Finland*
[g] *MAASTRO Lab, Maastricht University Medical Centre, the Netherlands*
[h] *Department of Toxicogenomics, Maastricht University Medical Centre, the Netherlands*

ARTICLE INFO

Keywords:
17β-estradiol
FP4643
17β-HSD-1 inhibitor
Ishikawa
Bioluminescence imaging

ABSTRACT

Endometrial cancer (EC) is the most common gynaecological tumor in developed countries and its incidence is increasing. Approximately 80% of newly diagnosed EC cases are estrogen-dependent. Type 1 17β-hydroxysteroid dehydrogenase (17β-HSD-1) is the enzyme that catalyzes the final step in estrogen biosynthesis by reducing the weak estrogen estrone (E1) to the potent estrogen 17β-estradiol (E2), and previous studies showed that this enzyme is implicated in the intratumoral E2 generation in EC. In the present study we employed a recently developed orthotopic and estrogen-dependent xenograft mouse model of EC to show that pharmacological inhibition of the 17β-HSD-1 enzyme inhibits disease development. Tumors were induced in one uterine horn of athymic nude mice by intrauterine injection of the well-differentiated human endometrial adenocarcinoma Ishikawa cell line, modified to express human 17β-HSD-1 in levels comparable to EC, and the luciferase and green fluorescent protein reporter genes. Controlled estrogen exposure in ovariectomized mice was achieved using subcutaneous MedRod implants that released either the low active estrone (E1) precursor or vehicle. A subgroup of E1 supplemented mice received daily oral gavage of FP4643, a well-characterized 17β-HSD-1 inhibitor. Bioluminescence imaging (BLI) was used to measure tumor growth non-invasively. At sacrifice, mice receiving E1 and treated with the FP4643 inhibitor showed a significant reduction in tumor growth by approximately 65% compared to mice receiving E1. Tumors exhibited metastatic spread to the peritoneum, to the lymphovascular space (LVI), and to the thoracic cavity. Metastatic spread and LVI invasion were both significantly reduced in the inhibitor-treated group. Transcriptional profiling of tumors indicated that FP4643 treatment reduced the oncogenic potential at the mRNA level. In conclusion, we show that 17β-HSD-1 inhibition represents a promising novel endocrine treatment for EC.

---

* Corresponding author. Dept. Obstetrics & Gynaecology, MUMC, P. Debyelaan 25, 6202AZ, Maastricht, the Netherlands.
E-mail address: sofia.xanthoulea@maastrichtuniversity.nl (S. Xanthoulea).
URL: https://og.mumc.maastrichtuniversity.nl/maastricht-endometrium-research-group (S. Xanthoulea).

[1] ENITEC: European Network Individualized Treatment Endometrial Cancer (www.esgo.org/network/enitec; within the European Society of Gynaecological Oncology: www.esgo.org).

[2] SX & GFJK contributed equally to the study.

https://doi.org/10.1016/j.canlet.2021.03.019
Received 14 December 2020; Received in revised form 4 March 2021; Accepted 16 March 2021
Available online 21 March 2021
0304-3835/© 2021 The Authors. Published by Elsevier B.V. This is an open access article under the CC BY license (http://creativecommons.org/licenses/by/4.0/).

1. Introduction

According to the GLOBOCAN 2018 database, endometrial cancer (EC) is the second most commonly diagnosed cancer and the fourth leading cause of death due to gynecological cancers among women worldwide, and accounted for ~90,000 deaths in 2018 [1]. Incidence of EC is rising rapidly, due to an increase in life expectancy and obesity, and consequently mortality is estimated to increase by 70% by 2040 worldwide [1,2].

Based on histological characteristics, EC has historically been classified into two main subtypes: Type I that are low-grade, hormone-receptor positive endometrioid ECs and have favourable prognosis, and type II ECs that are non-endometrioid, high-grade, hormone-receptor negative, frequently *TP53* mutated and have poor prognosis. Type I endometrioid ECs constitute up to 80% of the cases, and unopposed estrogen exposure is one of the most important risk factors. Nonetheless, although considered estrogen insensitive, increasing evidence supports the relevance of estrogen signaling for non-endometrioid Type II ECs as well [3]. In the last years, The Cancer Genome Atlas (TCGA) classification identified four molecular subgroups with distinct genomic aberrations, adding accuracy to the traditional dualistic (type I/II) view. Interestingly, steroid hormone receptor (estrogen -ER- and progesterone -PR) positivity is seen across all TCGA subgroups and ranges between 72 and 81% [4]. Therefore, although the current antihormonal therapy is restricted to few settings (i.e. fertility sparing and palliative therapy), these drugs bear great therapeutic potential in the treatment of EC and it is generally agreed upon that there is room for improvement regarding their use [5]. In fact, hormonal therapy administered to properly selected patients can be as effective as cytotoxic chemotherapy, but without the toxicity and less side effects, and at a much lower cost [6,7].

The availability of relevant preclinical models that can closely mimic the human disease is crucial for the advancement of research and the testing of novel drug candidates. We have previously reported the development of a novel orthotopic xenograft mouse model of EC that exhibits features similar to the human disease such as estrogen dependency, lymphovascular invasion (LVI) and metastatic spread, and thus is highly relevant [8]. In this model, tumors are induced in the same tissue as these occur in humans (orthotopic) and circulating estrogen levels are exogenously controlled by the subcutaneous implantation of estrogen releasing implants in ovariectomized mice.

In the current study, EC cells derived from the well-differentiated and estrogen sensitive human endometrial adenocarcinoma Ishikawa cell line were used to induce orthotopic EC in mice, and the in-vivo efficacy of the 17β-HSD-1 inhibitor FP4643 (a well characterized inhibitor of the enzyme 17β-hydroxysteroid dehydrogenase-1) was examined. By catalyzing the final step in estrogen biosynthesis - reducing the weak estrogen estrone (E1) to yield the potent estrogen 17β-estradiol (E2) - 17β-HSD-1 is responsible for the intratumoral E2 generation in human ECs [9,10]. Using primary tumors from patients ex-vivo we have previously shown that 17β-HSD-1 enzyme activity was inhibited by over 90% by FP4643[11]. In addition, in both in-vitro cell line models and in-vivo, using the chicken chorioallantoic membrane (CAM) model, the FP4643 inhibitor efficiently blocked 17β-HSD-1 enzyme activity, the generation of E2 from E1, and tumor proliferation [11].

We here show that also in-vivo, in the highly relevant orthotopic mouse model of EC, 17β-HSD-1 inhibition by FP4643 impairs EC growth by approximately 65% and leads to reduced lymphovascular invasion (LVI) and metastatic spread of tumor cells. Transcriptional profile analysis of tumor tissue indicated that 17β-HSD-1 inhibition by FP4643 was associated with downregulation, among others, of genes promoting cell migration or epithelial-to-mesenchymal transition, and upregulation of tumor suppressor genes.

2. Materials and methods

2.1. Ethics statement

All animal procedures were approved by the relative national authorities: the Netherlands National Committee for the protection of animals used for scientific purposes and the Central Authority for Scientific Procedures on Animals (protocol ID: PV 2017–013/AVD1070020174025); the National Animal Experimental Board (approval number ESAVI4199/04.10.07/2014). All procedures were performed according to the European Convention for the Protection of Vertebrates Used for Scientific Purposes.

2.2. Cell lines and tumor graft preparation

The human endometrial adenocarcinoma cell line Ishikawa (ECACC, Sigma-Aldrich, Zwijndrecht, The Netherlands) was previously modified in our laboratory to express firefly luciferase fused with green fluorescent protein (GFP) for non-invasive bioluminescence imaging (BLI), along with the human 17β-HSD-1 (clones Ishi-M3-HSDA and Ishi-M1-HSDB, referred to as clone 1 and clone 2 in the present study). A third clone, Ishi-M3-EVC, is identical to Ishi-M3-HSDA/M1-HSDB but lacks the 17β-HSD-1 open-reading-frame and was used as a genetic control in our experiments. Detailed description and characterization of the different clones is described elsewhere [11]. Cells were maintained in RPMI 1640 (Invitrogen, Carlsbad, CA) supplemented with sodium-pyruvate, L-glutamine, penicillin-streptomycin and 10% foetal bovine serum at 37 °C, 5% CO_2 in humidified air, and were tested negative for mycoplasma (MycoAlert, Promega, Madison, USA). Prior to experiments, cells were authenticated by short-tandem-repeat analyses as described earlier [11]. For orthotopic injections, cells at no more than 70% confluency were detached with Accutase (Invitrogen, Carlsbad, CA), pelleted, and resuspended in 30 μl ice-cold Matrigel (Basement Membrane Matrix; Becton Dickinson, Vianen, The Netherlands)/3×10^6 cells.

2.3. Orthotopic estrogen dependent endometrial cancer mouse model

Eight-week-old female athymic nude mice (Crl:NU(NCr)-Foxn1nu) were purchased from Charles River (‘s-Hertogenbosch, The Netherlands) and housed in groups of 2–3 animals in individually ventilated cages and under specified pathogen-free conditions. Low phytoestrogen diet (V1554-703 ssniff Spezialdiäten GmbH, Soest, DE) and water were both sterilised and provided ad libitum. EC cell injections were performed as described previously [8]. To exogenously provide steroids after ovariectomy, MedRods implants (PreclinApps Ltd, Raisio, Finland) were used. MedRods are polydimethylsiloxane cylinders covered by a silicone membrane to ensure constant release of the matrix embedded steroid for at least 10 weeks (depending on the compound) and were already successfully used in our model [8]. MedRods containing either vehicle only or E1 (releasing 0.02 μg of E1/day) were implanted subcutaneously in the back of the mice, in between the scapulae. Mice in the treatment arm received 25 mg/kg FP4643 inhibitor dissolved in 150 μl Phosal-50 (Lipoid GmbH, Ludwigshafen, Germany) by daily gavage. For analgesia, mice received 7.5 mg/kg carprofen (Norbrook Laboratories Ltd, Newry, UK) subcutaneously, pre-operatively and for the following two days. Compound FP4643 is earlier described by Messinger et al. as compound 21 [12].

2.4. Efficient delivery of the FP4643 inhibitor by oral gavage

Inhibitor FP4643 is a highly lipophilic compound and insoluble in aqueous vehicles. To test if oral gavage in Phosal-50 is an efficient delivery method, preliminary experiments were performed (Suppl. Fig. 5). Tumors were induced subcutaneously in the flank of E1 MedRod implanted mice (0.6 μg/day release), using 5×10^6 cells from clone 2

(Ishi-M1-HSDB) and allowed for 2.5 weeks of tumor growth. Mice were administered with inhibitor FP4643 (25 mg/kg) or placebo, via oral gavage (three times with 12 h intervals), and 4 h after the last gavage mice received a single intratumoral ^{3}H-E1 injection. Two minutes later tumors were excised and snap frozen to liquid nitrogen, homogenized, and the conversion of ^{3}H-E1 to ^{3}H-E2 was determined by HPLC-on-line radioactivity detector to measure the in vivo 17β-HSD-1 activity and inhibition. Data shown in Suppl. Fig. 5 indicate that oral gavage delivery of 25 mg/kg FP4643 inhibitor can efficiently reach the tumor and significantly inhibit intratumoral 17β-HSD-1 activity by approximately 25%.

2.5. Bioluminescence imaging (BLI)

Tumor growth was visualised by sequential BLI using the Andor iXon Ultra 897 camera that was mounted in the X-RAD 225Cx system (Precision X-ray Inc., North Branford, CT). Procedures were described earlier [8]. In short, mice were anaesthetised with isoflurane and injected intraperitoneally with 150 mg/kg D-Luciferin (Becton Dickinson, Vianen, The Netherlands), 10 min prior to imaging. Images were obtained using an Electron Multiplying charge-coupled device gain of 300, aperture of 0.5 and variable integration times, starting with 20s during the lag-phase and the initial time points, going down to 1s at humane-endpoints. The occurrence of a signal obtained with 20s integration time after the lag-phase (two weeks after tumor induction) was considered the baseline. Tumor growth was then monitored weekly by six planar images obtained at 0°, 45°, 90°, 180°, 270°, 315° angles (angle 0° corresponding to image from the top, dorsal side of the mouse). Images obtained from angles 270°–315° (left side) were used to compute the BLI signal intensity for tumors on the left uterine horn. Images obtained from the dorsal and ventral sides (0° and 180°) were used to monitor metastatic spread. BLI data was analyzed using ImageJ and the total photon flux was determined in the Region of Interest (ROI) located in the abdominal area corrected for background signal.

2.6. Histology and immunohistochemistry

Tissue biopsies were fixed in 3.7% formaldehyde, embedded in paraffin, and processed for histological examination. To assess metastatic spread in peritoneal and thoracic cavity organs, slides were prepared for histology every 200 μM to cover the complete depth of the tissue. Histology was determined by a gynecopathologist (LK) from 5 μm haematoxylin & eosin (Sigma-Aldrich, Zwijndrecht, The Netherlands) stained sections. For immunostaining of GFP, paraffin sections of 5 μm were deparaffinised, 2 × 5 min in xylene, and 2 × 5 min in 100% ethanol. The endogenous peroxidases were blocked by incubating 30 min in 0.3% H_2O_2 in methanol. For heat induced epitope retrieval, sections were boiled in citrate-buffer (pH 6.0) in a microwave for 20 min. After blocking (1% BSA/PBST) for 1 h at room temperature, staining with a rabbit polyclonal antibody TurboGFP(d) (1:300; Evrogen, Moscow, Russia) was performed overnight at 4 °C. To visualise the antibody, Chemate Envision and 3,3-diaminobenzidine (DAB) solution (Dako, Glostrup, Denmark) were used.

2.7. Steroid concentration by liquid-chromatography tandem mass spectrometry (LC-MS/MS)

Blood was collected from mice at sacrifice by heart puncture and steroid concentration in 150 μl serum was determined by LC-MS/MS after aqueous and lipidic phases were separated using 1 ml of toluene and reconstituted in 30% acetonitrile. The Agilent 1290 Rapid Resolution LC System (Agilent Technologies) was used for LC separation, whereas the mass analysis was carried out with an Agilent 6495 Jet Stream (AJS) ionization triple quadrupole mass spectrometer (Agilent Technologies). Agilent MassHunter Workstation software (Agilent Technologies) was used for data acquisition and quantification, and the Kinetex biphenyl (100 × 2.1 mm, 1.7u) was the column used. Further details and procedures were described earlier [13].

2.8. RNA isolation and sequencing

RNA was isolated from 10 cryosections of 10 μm from the middle of the primary tumor and after histological examination to ensure tumor presence but absence of mouse or necrotic tissue (Suppl. Fig. 4). The Qiagen RNeasy Mini Kit (Cat No./ID: 74104) with on-column DNase digestion using the RNase-Free DNase Set (Cat No./ID: 79254) was used, and RNA quality control and RNA-Seq using Poly-A selection (gene-expression profiling) was performed by GenomeScan B.V. (Plesmanlaan 1 d, 2333 BZ, Leiden, the Netherlands). Sample quality was determined using the Fragment Analyzer, and an RQN higher than 9.4 was required for further analyses. cDNA synthesis was performed for ligation with the sequencing adapters and PCR amplification of the resulting product. The quality and yield after sample preparation were measured with the Fragment Analyzer. The size of the resulting products was consistent with the expected size distribution (a broad peak between 300 and 500 bp). Clustering and DNA sequencing using the NovaSeq6000 was performed according to manufacturer's protocols (raw data are deposited in the European Nucleotide Archive (ENA) database with accession number: ArrayExpress accession E-MTAB-10338). The raw data files were quality assessed and trimmed with fastp (v. 0.20) using default parameters [14]. The trimmed reads were mapped to the human genome (Ensembl GRCh38 release 100) using STAR (v.2.7.3a) [15] and quantified with RSEM (v1.3.1) [16]. The raw counts were analyzed with DESeq2 using the standard parameters [17]. Genes with an adjusted p value below 0.05 (False discovery rate) were considered differentially expressed and selected for follow up analysis. Pathway enrichment analysis were carried out with ConsensusPathDB-human [18].

2.9. Statistics

Unless otherwise specified, statistical analysis was performed using Graphpad Prism. Data are expressed as mean ± SEM and analyzed by one-way ANOVA with Tukey's post-hoc test or with unpaired parametric *t*-test. A probability value of $p < 0.05$ was considered statistically significant ($^*p < 0.05$; $^{**}p < 0.01$; $^{***}p < 0.001$; $^{****}p < 0.0001$). Fisher exact test was used to analyse contingency tables/categorical data and Pearson's correlation test for correlation analyses.

3. Results

3.1. Orthotopic tumor induction and treatment groups

To study the efficacy of the 17β-HSD-1 inhibitor FP4643 on EC growth in vivo, we used a previously developed orthotopic mouse model of the disease. Tumors were induced by intrauterine injection of 3×10^6 Ishikawa-derived cells in the left uterine horn. These cells were previously modified to express the drug target 17β-HSD-1, in combination with the luciferase gene used for bioluminescent imaging (BLI). The luciferase gene was also fused with the green-fluorescent-protein gene (GFP) used for immunohistochemistry. To exclude any clonal effects that may have arisen during genetic manipulation of the cells, two different Ishikawa clones (Ishi-M3-HSDA and Ishi-M1-HSDB from now on referred to as clone 1 and clone 2, respectively) were used [11]. Previous studies on estrogen dependent cancer models showed that estrogens are required in the initial phase (lag phase), for successful tumor engraftment [19,20]. Therefore, to maintain the endogenous source of estrogens and to allow for Ishikawa cells to engraft, complete ovariectomy (OVX) was performed only after the completion of the lag phase (that lasted approximately 2 weeks; Fig. 1A). During tumor cell injection however, ipsilateral OVX of the left ovary was performed to avoid that, after tumor engraftment, tumor overgrowth would impede correct removal of the left ovary or that part of the tumor could be removed

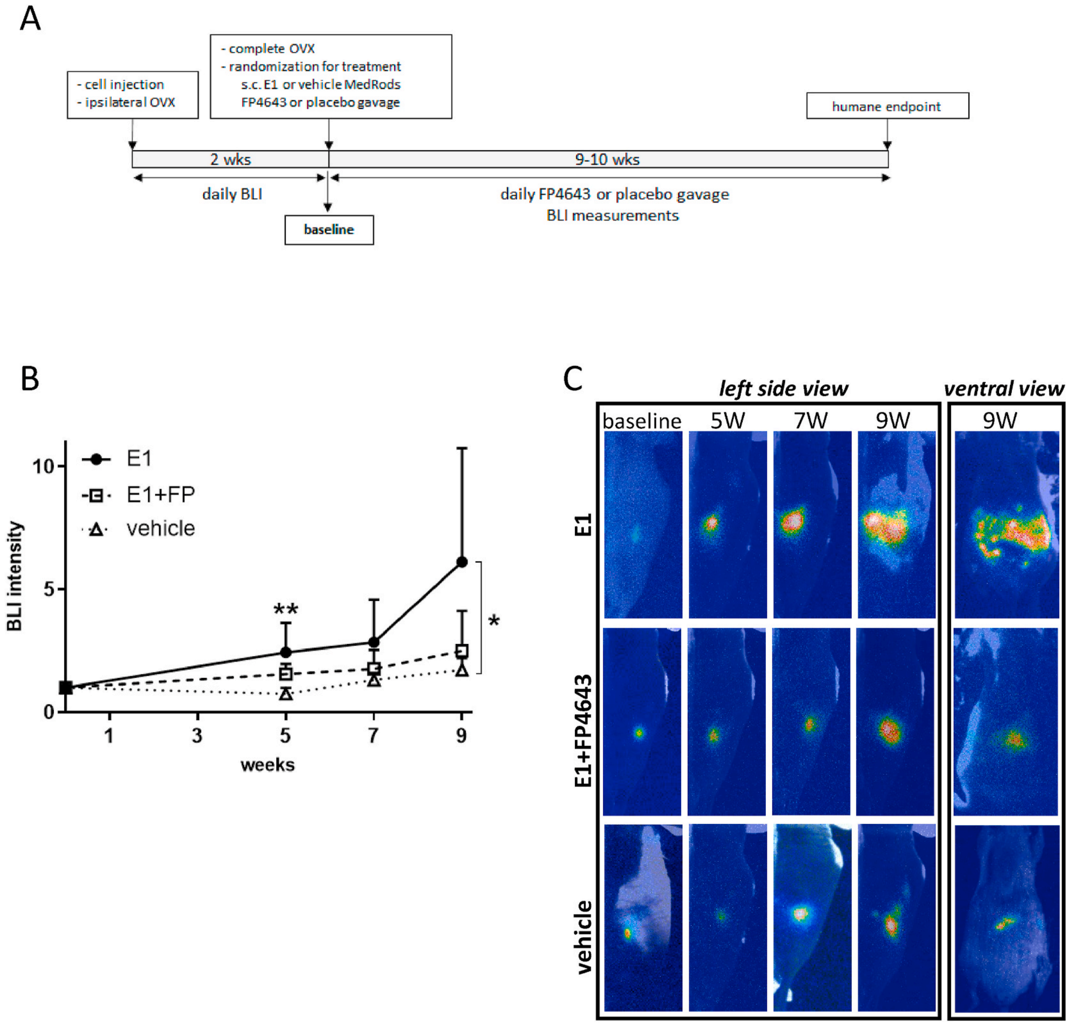

Fig. 1. Experimental timeline and in-vivo tumor growth. (A) Tumors were induced by orthotopic cell injection in the left uterine horn and at the same time ipsilateral OVX was performed. Two weeks later (after tumor engraftment confirmation and baseline definition by bioluminescence imaging - BLI), OVX was performed at the right uterine horn and mice were randomized for treatment. (B) BLI intensity quantification of clone 1 (Ishi-M3-HSDA)-induced tumors in the different groups ($n = 4–6$ mice/group), at baseline (0) and 5, 7, and 9 weeks later, $^{**}p < 0.01$ and $^{*}p < 0.05$ between E1 vs. vehicle at time-points 5 and 9 weeks respectively. (C) Representative BLI images of clone 1 (Ishi-M3-HSDA) tumor growth from the left side or ventral views at baseline and 5, 7, and 9 weeks later.

together with the ovary. Successful tumor engraftment was verified by a positive BLI signal (Fig. 1C; baseline). At this time point (set as baseline for tumor growth), mice with engrafted tumors were completely ovariectomized and randomized for treatment (Fig. 1A and Table 1).

An initial set of experiments was performed with mice injected with cells not expressing 17β-HSD-1 (empty vector clone 3-Ishi-M1-EVC) (Table 1) [11]. The use of this clone served as a negative genetic control, to exclude tumor growth after E1 administration in the absence of 17β-HSD-1 expression (Suppl. Fig. 1A, C). In addition, in these experiments we determined the dose of E1 released by MedRods that has no/minimal estrogenic/uterotrophic effects (as assessed by the minimal increase in uterine weight in E1 supplemented mice seen in Suppl. Fig. 1B) but was sufficient to induce tumor growth in the 17β-HSD-1-positive clones injected mice. Our previous studies showed that mice are very sensitive to even low amounts of E1 (most likely because of the absence of the steroid binding globulin), and E1 levels that are not sufficient to induce any estrogenic signal in humans, were able to elicit tumor and uterine growth in mice [8]. The dose of E1 was set to 0.02 μg/day resulting in approximately 15 pM serum E1 (Suppl. Fig. 1E).

Table 1

Number of mice used for each treatment.

	E1	E1+FP	vehicle[a]	vehicle + FP	E1+placebo[b]	E2
Clone 1 (Ishi-M3-HSDA)	9	8	8	6	3	–
Clone 2 (Ishi-M1-HSDB)	10	9	6	–	–	–
Clone 3 (Ishi-M1-EVC)	5	–	6	–	–	4

[a] with vehicle is indicated MedRods containing solvent alone without E1.

[b] with placebo is indicated oral gavage with Phosal-50 alone without FP4643.

For 17β-HSD-1 expressing Ishikawa clone 1 (Ishi-M3-HSDA), 9 mice were implanted with E1 releasing MedRods, 8 mice were implanted with E1 releasing MedRods and in addition, received daily oral gavage of 25 mg/kg FP4643 inhibitor (see M&M for dose determination), 8 mice were implanted MedRods releasing vehicle only (solvent without E1 - to ensure tumor growth was estrogen dependent), and an additional control group of 6 mice received vehicle only MedRods and daily oral gavage of 25 mg/kg of FP4643 (pharmacological control - to ensure the inhibitor had no estrogenic or potential adverse effects). To control for potential effects of the gavage procedure on the E1-induced tumor growth, an extra control group of mice ($n = 3$) was implanted with E1 MedRods and received a daily sham oral gavage of the FP4643 solvent Phosal-50 alone (E1 + placebo group) (Table 1). No side effects due to the gavage procedure were observed and tumors developed comparably to the E1 group (average tumor weight in mg ± SEM: 1577 ± 247 for the E1 group vs. 1107 ± 753 for the E1 + placebo group; *t*-test p value = 0.4; Suppl. Fig. 1D). For Ishikawa clone 2 (Ishi-M1-HSDB), 10 mice received E1 MedRods, 9 mice E1 MedRods + FP4643 gavage, and 6 mice vehicle only MedRods.

3.2. *17β-HSD-1 inhibition by FP4643 impairs tumor growth*

Mice were monitored regularly for body weight and tumor growth by BLI. No significant differences in body weights were observed between the groups (Suppl. Fig. 2A and B). BLI imaging indicated a gradual increase in tumor size that was more pronounced in the E1 group compared to the E1+FP4643 inhibitor or the vehicle only groups (Fig. 1B and C and Suppl. Fig. 2C for control groups). Mice were sacrificed when humane endpoints were reached, defined by a tumor volume of approximately 1500 mm^3 (assessed by BLI), and that corresponded to 9 weeks for clone 1 and 10 weeks for clone 2 from baseline (Fig. 1A). For both clones, mice in the E1 arm reached first the humane endpoint. At sacrifice, uteri, tumors and other organs were isolated and examined. Tumor weight for clone 1 (Fig. 2A) and clone 2 mice (Fig. 2B) indicated that E1 administration via the MedRods resulted in E1→E2 conversion by the 17β-HSD-1 expressing Ishikawa cells and tumor growth in the E1 group as compared to the vehicle only group. Administration of the FP4643 inhibitor resulted in 67% inhibition in tumor growth in clone 1 ($p = 0.0003$) and 62% in clone 2 mice ($p = 0.0042$) compared to the E1 group. Administration of the FP4643 inhibitor alone without E1 (vehicle + FP4643 group) confirmed the absence of tumor growth in the absence of E1. In addition to tumor weight, we measured the uterine weight of the mice. As shown in Fig. 2C and D, administration of E1 showed mild estrogenic/uterotrophic effects (shown by the increased uterine weight in the E1 and E1+FP4643 groups compared with the vehicle only group). This effect was slightly higher than what observed in mice harboring 17β-HSD-1-negative tumors (clone 3-Ishi-M1-EVC; Suppl. Fig. 1B) in which the mean uterine weight in E1 mice was around 60 mg compared with 100 mg in the 17β-HSD-1 expressing tumors. This could be caused by the contribution of both a direct mild uterotrophic effect of E1, and of an uterotrophic action of E2 produced in the tumor tissue and affecting the uterus via paracrine diffusion or via the circulation. No estrogenic effects on uterine growth of the FP4643

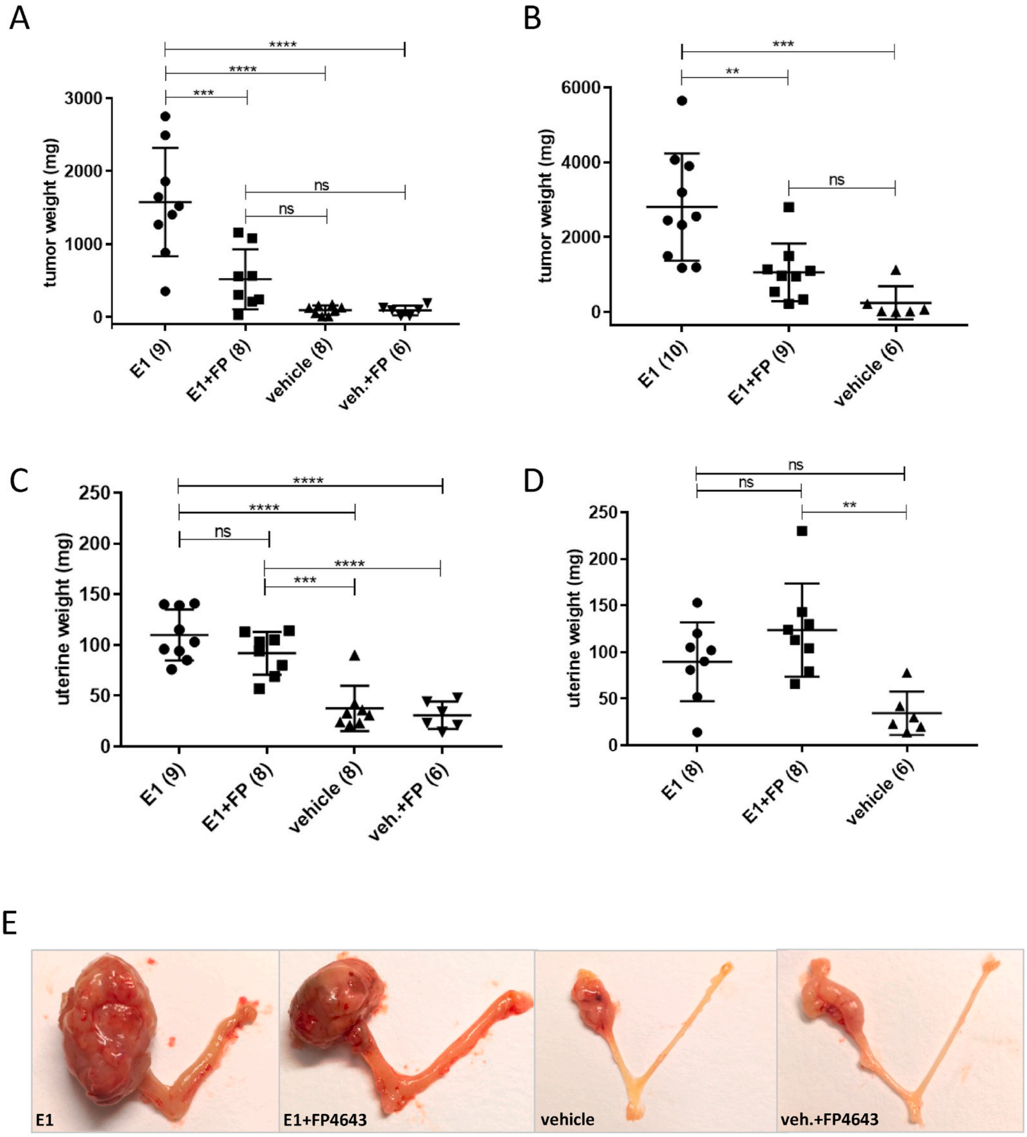

Fig. 2. FP4643 treatment inhibits E1-induced tumor growth. Tumor and uterine weights in (A, C) clone 1 (Ishi-M3-HSDA) and (B, D) clone 2 (Ishi-M1-HSDB) mice and (E) representative pictures of tumors and uteri at sacrifice. Numbers in parentheses represent the number of mice analyzed in each group. P values were calculated by one-way ANOVA with Tukey's post-hoc test (*$p < 0.05$; **$p < 0.01$; ***$p < 0.001$; ****$p < 0.0001$).

inhibitor alone (vehicle only + FP4643 group) could be observed (Fig. 2C).

Tumor histological analysis was performed by an experienced gynecopathologist (LK) (Fig. 3). Tumors showed an infiltrative growth of solid sheets and nests, although not frequently - probably due to the lack of a proper stroma cell support - and glandular structures were also seen. Cells were atypical and showed a disturbed nuclear-cytoplasmic ratio and hyperchromasia. Also, multiple mitotic figures were visible.

3.3. Steroid serum levels

Blood samples were collected at sacrifice and, in a subgroup of mice, we quantified serum levels of E1 and E2 by Liquid-Chromatography tandem Mass-Spectrometry (LC-MS/MS). As expected, mice from the vehicle only group (not receiving E1), had undetectable serum levels of E1 or E2, whereas mice implanted with E1 MedRods showed detectable levels of E1 (around 15 pM) (Fig. 4A). Serum E2 levels in E1 implanted mice were readily detectable (around 14 pM), indicating that intratumoral E2 generation influenced the systemic E2 levels. E2 dropped below detection limit in the E1+FP4643 treatment group (Fig. 4B) indicating efficient inhibition of E1→E2 conversion by FP4643.

3.4. 17β-HSD-1 inhibition by FP4643 inhibits metastatic spread

Metastatic spread was assessed post-mortem by macroscopic inspection of the different organs at sacrifice, by ex-vivo BLI of organs of the peritoneal cavity and the heart and lungs (Fig. 5A, B and C), and by histological confirmation (Fig. 6). The extent of metastatic spread and number of BLI positive organs correlated with tumor size (Pearson's correlation coefficient $r = 0.54$; $p < 0.0001$; 95% CI 0.32 to 0.70; Suppl. Fig. 3). Metastatic spread (both local in the peritoneal cavity and distant to the thoracic cavity) was highest in the E1 group and was inhibited by treatment with FP4643 (Fig. 5D and E). In particular, a total of 9 out of 19 mice in the E1 group showed distant metastases to the lungs compared with 2 out of 17 mice in the E1+FP4643 inhibitor group ($p = 0.03$ by Fischer's exact test). Metastatic spread and lympho-vascular invasion (LVI) of tumor cells were also validated histologically by an expert gynecopathologist (LK), and further confirmed by immunohistochemistry, using an antibody against GFP, which allowed to distinguish tumor cells (harbouring the luciferase/GFP fusion gene) from the surrounding mouse tissue (Fig. 6). In line with the metastatic spread, LVI positivity was highest in E1-treated mice and was inhibited by FP4643 treatment (12/13 for E1 group vs. 6/13 for E1+FP4643 group; $p = 0.03$ by Fischer's exact test).

3.5. 17β-HSD-1 inhibition by FP4643 is associated with a reduced oncogenic profile at the mRNA level

To better characterize the cellular effects of the 17β-HSD-1 inhibitor FP4643, we determined the transcriptional profile of tumors exposed to E1 alone or E1 in the presence of the inhibitor. Since tumors may be heterogenous (core versus margins) and may contain important inflammatory/necrotic foci, to avoid potential associated biases, tumors were cut in half and slices for RNA isolation were obtained from the middle part (largest diameter). This ensured that the tumor specimens used for RNA-seq analyses originated from similar areas of the primary tumor. In addition, prior to RNA isolation, histologic analyses confirmed that samples contained tumor tissue, no visible mouse endometrial tissue, and no necrotic foci (Suppl. Fig. 4). The raw RNA-seq reads were aligned to both the human and mouse genomes and results confirmed

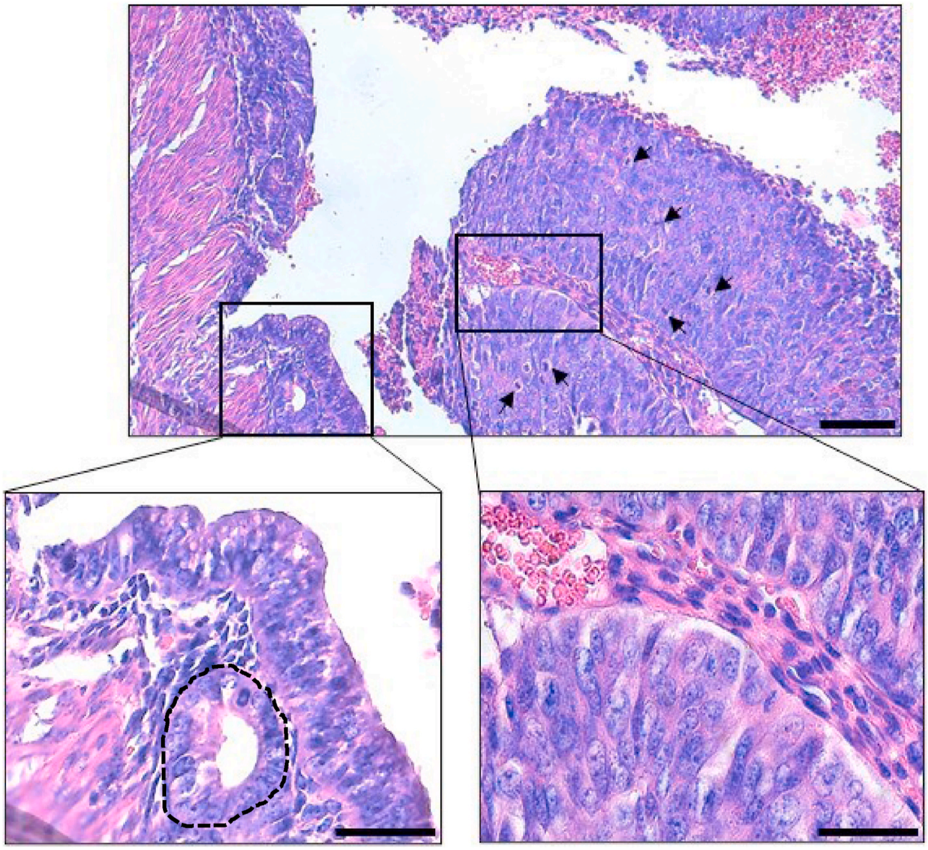

Fig. 3. Primary tumor histology. Representative images of primary tumor that recapitulates a well-differentiated human EC. A solid tumor structure is predominant and glandular organizations of the epithelial cells are visible (dashed line in left inset). Nuclei are hypochromatic (see insets). Mitotic figures are indicated with arrows. Scale bars 100 μm and 50 μm in insets.

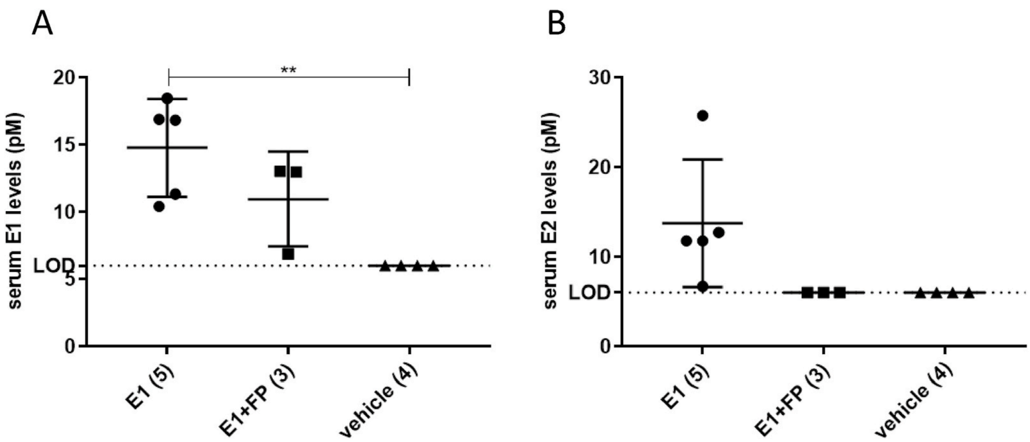

Fig. 4. Estrone (E1) and estradiol (E2) levels in serum. Serum levels of (A) E1 and (B) E2 at sacrifice, as determined by Liquid-Chromatography tandem Mass-Spectrometry (LC-MS/MS). E2 levels in the E1+FP4643 and vehicle groups are below detection limit (6pM). **$p < 0.01$.

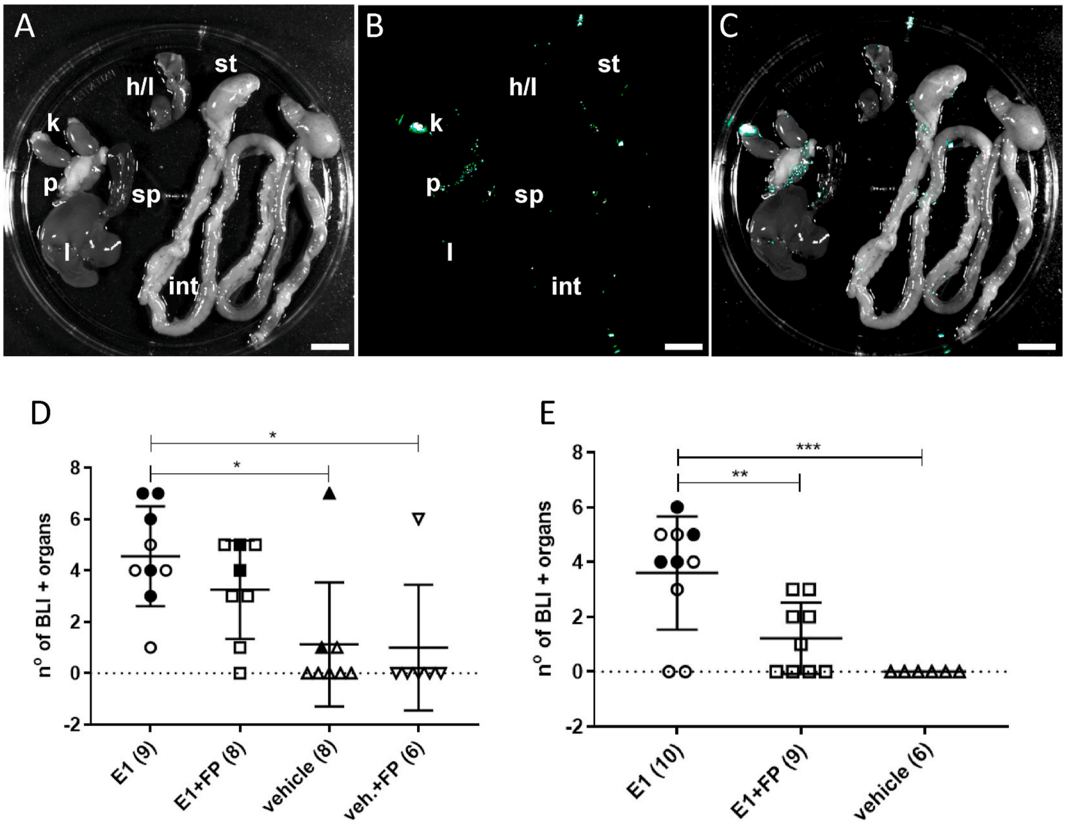

Fig. 5. FP4643 treatment inhibits metastatic spread. Ex vivo BLI performed to organs excised at sacrifice, to determine the extent of metastatic spread. (A) white light image, (B) BLI indicating luciferase-expressing tumors cells, and (C) merged images (scale bars 1 cm). Major organs like liver (l), pancreas (p), kidneys (k), spleen (sp), intestines (int), heart and lungs (h/l) and stomach (st) were examined. Extent of metastatic spread as assessed by the number of BLI positive organs for (D) clone 1 (Ishi-M3-HSDA) and (E) clone 2 (Ishi-M1-HSDB) mice. Black symbols represent mice that exhibited lung metastases. *$p < 0.05$; **$p < 0.01$; ***$p < 0.001$.

that the human-aligned fraction represented in all samples the largest part of the reads. Each sample had at least 10 × 10^6 reads relative to the human genome, thus ensuring sufficient coverage for further analyses (Suppl. Fig. 4). We next confirmed that a panel of genes associated with endometrium/endometrial cancer features was expressed (Fig. 7A and B). This panel included endometrial markers (like ERS1, PGR, AR, PTEN, IGF1R, FGFR1), epithelial markers (like CDH1, EPCAM), and the drug target 17β-HSD-1 (HSD17B1), confirming that the tumor at endpoint maintained the main phenotypic characteristics of the cells used for tumor induction. We also assessed the expression of genes encoding for the major enzymes involved in the local steroid metabolism, and confirmed previous data that showed low/no expression of most of these enzymes in the Ishikawa cells like HSD17B2, CYP19A1 (ARO) and CYP17A1 (Fig. 7B). Differential expression analysis showed that 51 genes were down- and 81 upregulated by FP4643, with a pattern that was consistent with an overall antitumor effect as FP4643 treatment suppressed several tumor promoting genes and induced tumor suppressing genes (Suppl. Table 1). Top 10 downregulated genes (Fig. 7C) included genes associated with tumorigenicity (COLCA1, KITLG, PHF8, KAT2B, SLC1A5, CPM), whereas top 10 upregulated genes included

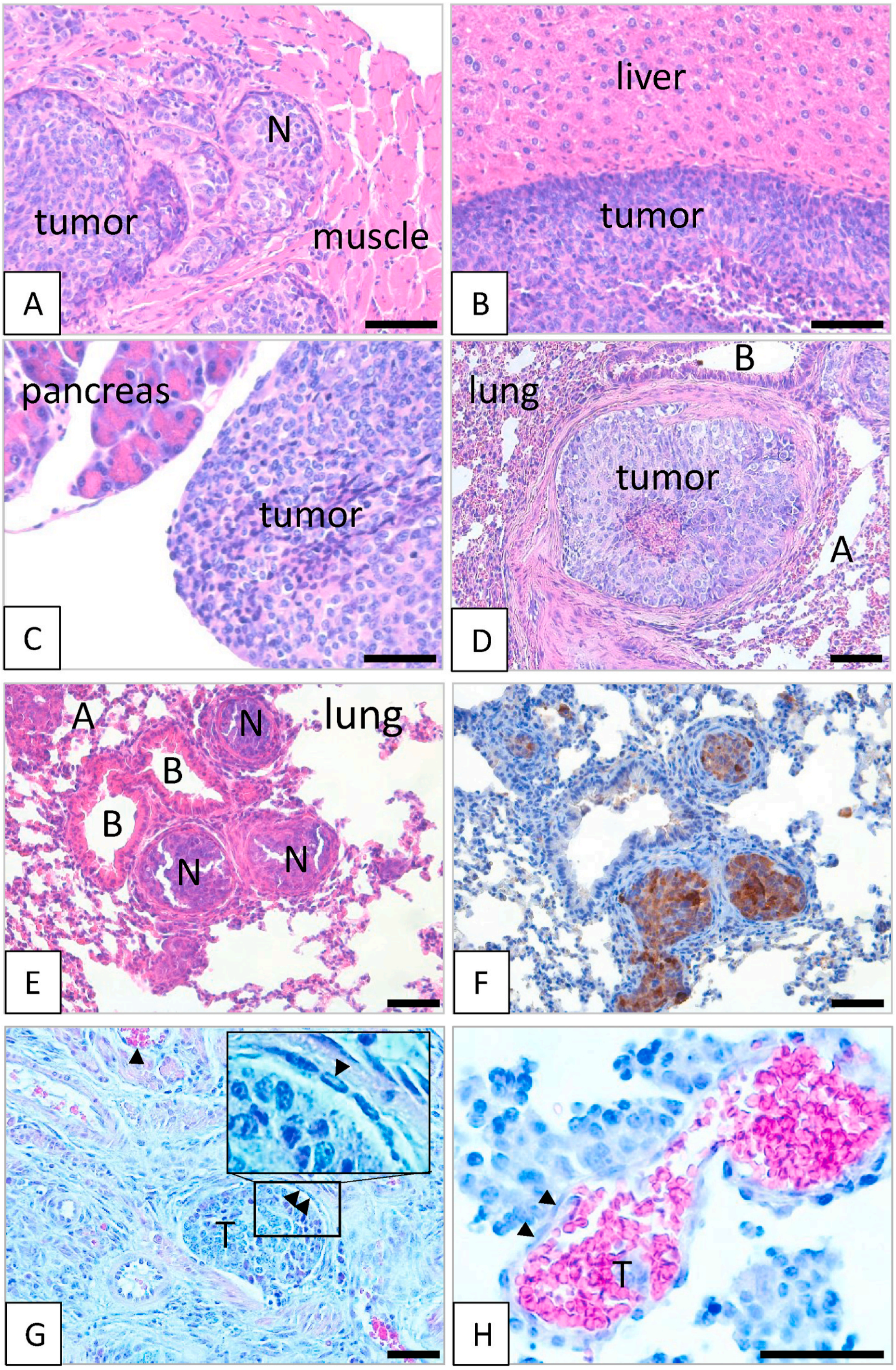

Fig. 6. Histological/immunohistochemical confirmation of metastatic spread. (A–D) Metastatic spread was confirmed histologically in peritoneal and thoracic cavities (H&E staining). Tumor invasion in the form of nested structures (N) in (A) iliopsoas muscle, (B) liver, (C) pancreas, (D) lungs (A = alveoli and B = bronchiole). (E–F) H&E staining of nested tumor structures (N) (A = alveoli and B = bronchiole), and GFP immunohistochemistry (F) used to confirm metastatic spread of the induced primary tumor to the lungs. (G–H) Representative images of LVI with tumor cells (T) clearly visible in blood vessels (endothelial cells are indicated by black arrowheads). Scale bars 100 μm.

tumor suppressors like TGFBI, DIRAS3, DUSP6. Pathway analysis showed that pathways involved in cell-cell interactions were strongly enriched (CAM molecules), together with those involved in cancer (‘Sprouty regulation of tyrosine kinase signals’, transcriptional regulation in cancer; Table 2).

A complete overview of up and down regulated genes with their putative involvement in cancer is given in Suppl. Table 1. The RNA reads mapping to the mouse genome were not further analyzed since their number was too low.

4. Discussion

In the present study we tested preclinically the therapeutic efficacy for EC treatment of the potent and specific 17β-hydroxysteroid dehydrogenase-1 (17β-HSD-1) inhibitor, FP4643, in a highly relevant orthotopic EC xenograft mouse model. FP4643 inhibits the 17β-HSD-1 enzyme that catalyzes the final step in estradiol biosynthesis. We show that FP4643 treatment reduces by up to 65% tumor growth, by up to 35% distal metastases and by over 45% LVI, hence, impacting favourably on the tumor growth and staging.

We used a mouse cancer model that we specifically developed to recapitulate the main features of human EC, such as orthotopic location,

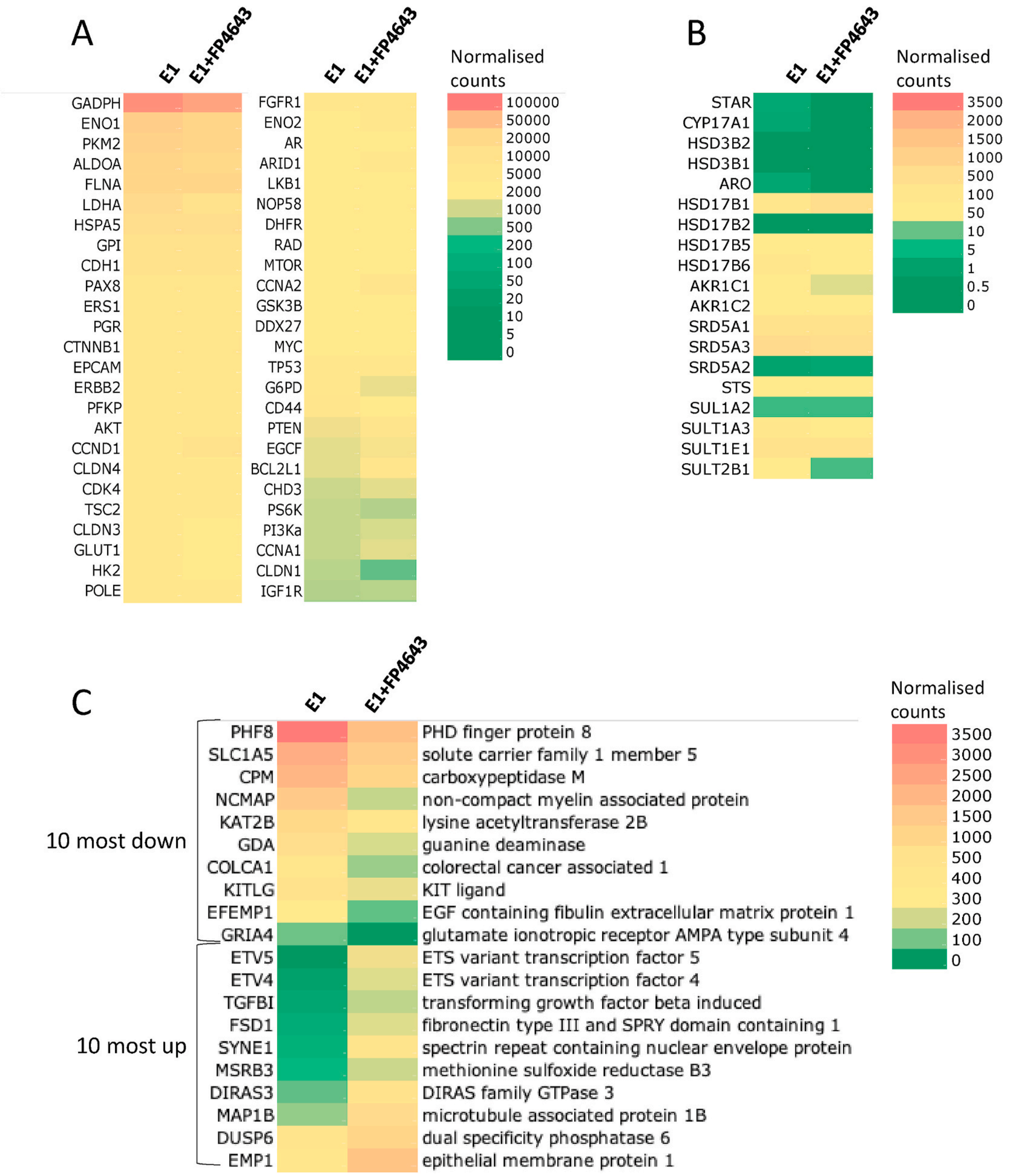

Fig. 7. RNA-seq profiles of E1 and E1+FP4643 treated tumors. Expression profiling of tumors exposed to E1 or E1+FP4643 (n = 3/group) was determined. (A,B) Tumors express a panel of endometrial/endometrial cancer genes like ERS1, PGR, AR, PTEN, epithelial markers like CDH1, EPCAM, and 17β-HSD-1 (HSD17B1), confirming the phenotypic characteristics of orthotopically injected cells. (B) Expression of genes encoding for enzymes of the local steroid metabolism. (C) Top 10 downregulated genes include tumor promoting genes like COLCA1, KITLG, PHF8, KAT2B, SLC1A5, CPM while top 10 upregulated genes include tumor suppressors like TGFBI, DIRAS3, DUSP6.

estrogen-dependent tumor growth, metastatic spread to peritoneal organs and lungs, and invasion of the lympho-vascular space [8]. The transcriptional profile of tumor tissues confirmed that induced lesions maintained the expression of genes relevant to an epithelial phenotype, and biomarkers of endometrial glandular cells (steroid hormone receptor expression like ERS1, PGR, GR, AR, adhesion molecules like CDH1, EPCAM, and other biomarkers like PTEN). In addition, expression profiling of tumors indicated that the FP4643 inhibitor suppressed the carcinogenic potential: in line with the diminished metastatic spread and LVI, pathways involved in cell-cell interactions were affected, including NrCAM interactions, beta integrin pathways and the Sprouty regulation of tyrosine kinase signals that modulates the action of several mitogens involved in cancer [21,22]. The 10 most down-regulated genes by FP4643 treatment included promoters of cell migration (KITLG [23]), of epithelial-to-mesenchymal transition (shown in breast cancer for PHF8 [24]), genes involved in cancer (COLCA1 and CPM [25,26]), KAT2B, a regulator of NOTCH that is overexpressed in cervical cancer [27], and SLC1A5, the transporter of glutamine that commonly becomes a conditionally essential amino acid in cancer including EC [28]. Top 10 upregulated genes included tumor suppressors like TGFBI [29], DIRAS3 [30], DUSP6 [31], genes associated with progesterone response (MAPB1) [32] and genes frequently altered in EC (SYNE1 [33,34]). Two members of the Ets family of transcription factors with oncogenic action (ETV4 and ETV5) were also among the top 10 upregulated genes. These transcription factors are essential for the activation of the estrogen signalling by the estrogen receptor, hence their upregulation could be secondary to a prolonged low estrogenic environment [35,36].

The 17β-HSD-1 enzyme is highly expressed in endocrine organs (ovary and placenta), the main sites of estrogen synthesis. However, local 17β-HSD-1 expression in peripheral organs is responsible for

Table 2
Enriched pathway-based sets.

Pathway	p-value	overlap	size	source	Pathway ID
Trafficking of AMPA receptors[a]	$5\ e^{-05}$	GRIP2; CACNG4; DLG4; GRIA4	31	Reactome	R-HSA-399719
NrCAM interactions	*0.001*	DLG4; NRP2	7	Reactome	R-HSA-447038
Beta1 integrin cell surface interactions	*0.001*	TGFBI; FN1; JAM2; ITGA7	66	PID	integrin1_pathway
Ethanol degradation II	*0.001*	ACSS1; ADH1C	8	HumanCyc	PWY66-21
Purine nucleotides degradation Purine catabolism	*0.003*	GDA; NT5E	12	HumanCyc Reactome	PWY-6353 R-HSA-74259
Ethanol oxidation	*0.003*	ACSS1; ADH1C	12	Reactome	R-HSA-71384
Steroid biosynthesis *Homo sapiens* Cholesterol biosynthesis (I, II and III)	*0.007*	EBP; FDFT1	19	KEGG HumanCyc	path:hsa00100 PWY66-341
Sprouty regulation of tyrosine kinase signals	*0.008*	SPRY2; SPRY4	20	BioCarta	sprypathway
Transcriptional mis-regulation in cancer	*0.009*	ETV1; HMGA2; DUSP6; ETV5; ETV4	186	KEGG	hsa05202

[a] **same genes also in the following pathways:** Glutamate binding, activation of AMPA receptors and synaptic plasticity; LGI-ADAM interactions; unblocking of NMDA receptor, glutamate binding and activation; trafficking of GluR2-containing AMPA receptors; synaptic adhesion-like molecules (R-HSA-5682910; R-HSA-416993; R-HSA-8849932; R-HSA-438066).

regulating the intra-tissue estrogen levels, for fine-tuning the downstream signalling, and for sustaining growth of cancer as well as other estrogen-dependent disorders [10,37,38]. Pharmacological inhibition of 17β-HSD-1 proved of therapeutic potential in preclinical models of breast cancer [20], endometrial hyperplasia [39], endometriosis [40], and our team also showed the therapeutic potential of this drug target using in-vitro models and a CAM model of EC [11]. Interestingly, a derivative of the compound used in these preclinical studies has entered in 2018 the clinical phase in humans for the treatment of endometriosis [37]. Recently, also genetic knock-down approaches of 17β-HSD-1 showed promising results on breast cancer [41], thus opening to the possibility of targeting this metabolism through multiple and alternative methods.

From a clinical perspective, hormonal drugs in the form of anti-estrogens or progestins are indicated for fertility preservation (accounting for about 5% of the total cases) or as palliative treatment in case of advanced stage or recurrent EC that accounts for up to 30% of the patients. Results on hormonal drugs in the adjuvant setting show no benefit, but data is scarce, and the quality of the studies does not allow taking definitive conclusions [42]. Response rates in fertility sparing or metastatic/recurrent EC are almost 50% or range between 20 and 50%, respectively, with a number of patients experiencing long-lasting responses (reviewed in Refs. [43,44]). It is overall agreed that hormonal drugs are under-exploited in the treatment of EC, also in view of their safety profile. Of note, although traditionally the estrogen-dependency was associated exclusively with type I endometrioid EC and not with type II lesions, a recent study on over 14000 cases and 35000 controls indicated that the same risk factors typically related to estrogen over-exposure (parity, oral contraceptive use, age at menarche and diabetes) also characterize the aggressive type II ECs, that more frequently than type I lesions need medical treatments [45]. This is confirmed by the novel molecular classification of EC (TCGA/Promise), that shows that estrogen and progesterone receptor positivity is seen across all four subtypes (ranging between 72 and 81%) and implies that a proportion of all EC types may respond to hormonal drugs [4,46].

The current use of hormonal drugs in the treatment of EC can be improved primarily by identifying responsive patients and by preventing/overcoming the development of drug insensitivity [5,42,43,47,48]. It is encouraging that a number of ongoing initiatives aim at tackling these major issues. The PROMOTE study (ClinicalTrials.gov: NCT03621904) is developing algorithms to predict the response to hormonal drugs using molecular pathway analyses, an approach already proven to be of prognostic value in EC and to predict drug response in breast cancer [7]. Since response to hormonal drugs may be compromised by additional survival pathways, recent/ongoing trials identified ways to improve the sensitivity of patients to hormonal drugs by their combination with other targeted treatments. For example, a phase II singe arm trial in advanced stage EC indicated that inhibition of the mTOR pathway could improve the response to an aromatase inhibitor (32% of the patients responded to the treatment [49]), and the superiority of this regimen compared with standard hormonal therapy was confirmed in a subsequent randomized controlled trial (unpublished; study results available at ClinicalTrial.gov: NCT02228681); inhibition of CDK is also of therapeutic value in combination with hormonal therapies (unpublished; study results available at ClinicalTrial.gov: NCT02657928). Results are awaited from a number of ongoing studies exploring the combination of hormonal therapies with agents blocking CDK4/6 (Palbociclib; NCT02730429); mTOR and CDK (Everolimus plus Ribociclib; NCT03008408); dual mTORC1/mTORC2 inhibitor (NCT02730923); with agents enhancing the hormone receptor expression like sodium cridanimod (NCT03077698).

In conclusion, we show here that pharmacologic inhibition of 17β-HSD-1 can be a novel promising target to treat EC. In contrast to traditional hormonal drugs that either block/modulate the receptor (tamoxifen/fulvestrant) or reduce the serum estrogen levels (aromatase inhibitor), 17β-HSD-1 inhibitor FP4643 reduces the local synthesis and availability of estrogens. The first drug entering the clinical phase for EC (phase II) and that, similar to FP4643, reduces the local availability of estrogens was Irosustat, an inhibitor of the enzyme steroid sulfatase. Although Irosustat as monotherapy was not superior to the comparator (progestin), it showed therapeutic benefit, and patient response might be improved by better tailoring the drug to responsive patients [37]. The availability and the ongoing development of novel hormonal drugs is a promising clinical scenario since, being able to offer EC patients hormonal drugs with alternative therapeutic mechanisms, will allow the implementation of multimodal treatment strategies. These, in addition to the combinational drug regimens described above, can diminish the development of drug insensitivity.

Funding

The present study was sponsored by the Dutch Cancer Society (KWF Kankerbestrijding: www.kwf.nl), contract number UM-13-5782 granted to AR.

Author contributions

Pathology assessment: LK; Image analysis: SX, GFJK, BD, EDA, YW; Steroid profiling by LC-MS/MS: NS, SA, MRH, PK; RNA-seq analysis: FC.

Sofia Xanthoulea: conceptualization, methodology, writing/original draft preparation, supervision **Gonda Konings:** conceptualization, methodology, writing-review & editing **Niina Saarinen:** methodology, writing-review & editing **Bert Delvoux:** methodology, supervision, writing-review & editing **Loes FS Kooreman:** validation, writing-review & editing **Pasi Koskimies:** conceptualization, validation, writing-review & editing **Merja R Häkkinen:** methodology, writing-review & editing **Seppo Auriola:** conceptualization, writing-review & editing **Elisabetta D'Avanzo:** methodology **Youssef Walid:** methodology

Frank Verhaegen: resources **Natasja G Lieuwes:** methodology **Florian Caiment:** formal analysis **Roy Kruitwagen:** conceptualization, resources **Andrea Romano:** conceptualization, methodology, writing/original draft preparation, supervision, funding acquisition

Declaration of interests

The authors declare the following financial interests/personal relationships which may be considered as potential competing interests: Pasi Koskimies and Niina Saarinen are employees of Forendo Pharma Ltd. No additional conflict of interest is declared.

Acknowledgments

The authors are grateful the members of the animal care units of Maastricht University, University of Turku and TCDM personnel. The Kuopio mass spectrometry facility is supported by Biocenter Finland and Biocenter Kuopio.

Appendix A. Supplementary data

Supplementary data to this article can be found online at https://doi.org/10.1016/j.canlet.2021.03.019.

Abbreviations

17β-HSD-1	17β-hydroxysteroid dehydrogenase
BLI	Bioluminescence imaging
E1	Estrone
E2	17β-estradiol
EC	Endometrial cancer
GFP	Green fluorescent protein
LC-MS/MS	Liquid chromatography tandem mass spectrometry
LVI	Lymphovascular invasion
OVX	Ovariectomy

References

[1] F. Bray, J. Ferlay, I. Soerjomataram, R.L. Siegel, L.A. Torre, A. Jemal, Global cancer statistics 2018: GLOBOCAN estimates of incidence and mortality worldwide for 36 cancers in 185 countries, CA A Cancer J. Clin. 68 (6) (2018) 394–424.
[2] J.E.M. Ferlay, F. Lam, M. Colombet, L. Mery, M. Piñeros, A. Znaor, I. Soerjomataram, F. Bray, Global Cancer Observatory: Cancer Tomorrow, International Agency for Research on Cancer, Lyon, France, 2018. Available from: https://gco.iarc.fr/tomorrow. accessed 06042020.
[3] V.W. Setiawan, H.P. Yang, M.C. Pike, et al., Type I and II endometrial cancers: have they different risk factors? J. Clin. Oncol. 31 (20) (2013) 2607–2618.
[4] A.N. Karnezis, S. Leung, J. Magrill, et al., Evaluation of endometrial carcinoma prognostic immunohistochemistry markers in the context of molecular classification, J Pathol Clin Res 3 (4) (2017) 279–293.
[5] A.E. Derbyshire, N. Ryan, E.J. Crosbie, Biomarkers needed to predict progestin response in endometrial cancer, BJOG 124 (10) (2017) 1584.
[6] M.J. Carlson, K.W. Thiel, K.K. Leslie, Past, present, and future of hormonal therapy in recurrent endometrial cancer, Int J Womens Health 6 (2014) 429–435.
[7] W.J. van Weelden, L.J.M. van der Putten, M.A. Inda, et al., Oestrogen receptor pathway activity is associated with outcome in endometrial cancer, Br. J. Canc. 123 (5) (2020) 785–792.
[8] G.F. Konings, N. Saarinen, B. Delvoux, et al., Development of an image-guided orthotopic xenograft mouse model of endometrial cancer with controllable estrogen exposure, Int. J. Mol. Sci. 19 (9) (2018).
[9] K.M. Cornel, R.F. Kruitwagen, B. Delvoux, et al., Overexpression of 17beta-hydroxysteroid dehydrogenase type 1 increases the exposure of endometrial cancer to 17beta-estradiol, J. Clin. Endocrinol. Metab. 97 (4) (2012) E591–E601.
[10] K.M.C. Cornel, M.Y. Bongers, R. Kruitwagen, A. Romano, Local estrogen metabolism (intracrinology) in endometrial cancer: a systematic review, Mol. Cell. Endocrinol. 489 (2019) 45–65.
[11] G.F. Konings, K.M. Cornel, S. Xanthoulea, et al., Blocking 17beta-hydroxysteroid dehydrogenase type 1 in endometrial cancer: a potential novel endocrine therapeutic approach, J. Pathol. 244 (2) (2018) 203–214.
[12] J. Messinger, B. Husen, P. Koskimies, et al., Estrone C15 derivatives–a new class of 17beta-hydroxysteroid dehydrogenase type 1 inhibitors, Mol. Cell. Endocrinol. 301 (1–2) (2009) 216–224.
[13] M.R. Hakkinen, T. Heinosalo, N. Saarinen, et al., Analysis by LC-MS/MS of endogenous steroids from human serum, plasma, endometrium and endometriotic tissue, J. Pharmaceut. Biomed. Anal. 152 (2018) 165–172.
[14] S. Chen, Y. Zhou, Y. Chen, J. Gu, fastp: an ultra-fast all-in-one FASTQ preprocessor, Bioinformatics 34 (17) (2018) i884–i890.
[15] A. Dobin, C.A. Davis, F. Schlesinger, et al., STAR: ultrafast universal RNA-seq aligner, Bioinformatics 29 (1) (2013) 15–21.
[16] B. Li, C.N. Dewey, RSEM: accurate transcript quantification from RNA-Seq data with or without a reference genome, BMC Bioinf. 12 (2011).
[17] M.I. Love, W. Huber, S. Anders, Moderated estimation of fold change and dispersion for RNA-seq data with DESeq2, Genome Biol. 15 (12) (2014) 550.
[18] A. Kamburov, U. Stelzl, H. Lehrach, R. Herwig, The ConsensusPathDB interaction database: 2013 update, Nucleic Acids Res. 41 (Database issue) (2013) D793–D800.
[19] B. Husen, K. Huhtinen, M. Poutanen, L. Kangas, J. Messinger, H. Thole, Evaluation of inhibitors for 17beta-hydroxysteroid dehydrogenase type 1 in vivo in immunodeficient mice inoculated with MCF-7 cells stably expressing the recombinant human enzyme, Mol. Cell. Endocrinol. 248 (1–2) (2006) 109–113.
[20] B. Husen, K. Huhtinen, T. Saloniemi, J. Messinger, H.H. Thole, M. Poutanen, Human hydroxysteroid (17-beta) dehydrogenase 1 expression enhances estrogen sensitivity of MCF-7 breast cancer cell xenografts, Endocrinology 147 (11) (2006) 5333–5339.
[21] J.C. Cheng, H.M. Chang, S. Xiong, W.K. So, P.C. Leung, Sprouty2 inhibits amphiregulin-induced down-regulation of E-cadherin and cell invasion in human ovarian cancer cells, Oncotarget 7 (49) (2016) 81645–81660.
[22] B.E. Celik-Selvi, A. Stutz, C.E. Mayer, J. Salhi, G. Siegwart, H. Sutterluty, Sprouty3, Sprouty4, Two members of a family known to inhibit FGF-mediated signaling, exert opposing roles on proliferation and migration of glioblastoma-derived cells, Cells 8 (8) (2019).
[23] S. Yang, W.S. Li, F. Dong, et al., KITLG is a novel target of miR-34c that is associated with the inhibition of growth and invasion in colorectal cancer cells, J. Cell Mol. Med. 18 (10) (2014) 2092–2102.
[24] P. Shao, Q. Liu, P.K. Maina, et al., Histone demethylase PHF8 promotes epithelial to mesenchymal transition and breast tumorigenesis, Nucleic Acids Res. 45 (4) (2017) 1687–1702.
[25] V.D. Peltekova, M. Lemire, A.M. Qazi, et al., Identification of genes expressed by immune cells of the colon that are regulated by colorectal cancer-associated variants, Int. J. Canc. 134 (10) (2014) 2330–2341.
[26] C.J. Denis, A.M. Lambeir, The potential of carboxypeptidase M as a therapeutic target in cancer, Expert Opin. Ther. Targets 17 (3) (2013) 265–279.
[27] T. Liu, X. Wang, W. Hu, et al., Epigenetically down-regulated acetyltransferase PCAF increases the resistance of colorectal cancer to 5-fluorouracil, Neoplasia 21 (6) (2019) 557–570.
[28] W.J. Zhou, J. Zhang, H.L. Yang, et al., Estrogen inhibits autophagy and promotes growth of endometrial cancer by promoting glutamine metabolism, Cell Commun. Signal. 17 (1) (2019) 99.
[29] Y. Zhang, G. Wen, G. Shao, et al., TGFBI deficiency predisposes mice to spontaneous tumor development, Canc. Res. 69 (1) (2009) 37–44.
[30] D.B. Badgwell, Z. Lu, K. Le, et al., The tumor-suppressor gene ARHI (DIRAS3) suppresses ovarian cancer cell migration through inhibition of the Stat3 and FAK/Rho signaling pathways, Oncogene 31 (1) (2012) 68–79.
[31] M.J. Fan, S.M. Liang, P.J. He, X.B. Zhao, M.J. Li, F. Geng, Dusp6 inhibits epithelial-mesenchymal transition in endometrial adenocarcinoma via ERK signaling pathway, Radiol. Oncol. 53 (3) (2019) 307–315.
[32] C. Berger, N. Boggavarapu, E. Norlin, et al., Molecular characterization of PRM-associated endometrial changes, PAEC, following mifepristone treatment, Contraception 98 (4) (2018) 317–322.
[33] S. Chava, R. Gupta, Identification of the mutational landscape of gynecological malignancies, J. Canc. 11 (16) (2020) 4870–4883.
[34] T.A. O'Mara, D.M. Glubb, J.N. Painter, et al., Comprehensive genetic assessment of the ESR1 locus identifies a risk region for endometrial cancer, Endocr. Relat. Canc. 22 (5) (2015) 851–861.
[35] E. Colas, L. Muinelo-Romay, L. Alonso-Alconada, et al., ETV5 cooperates with LPP as a sensor of extracellular signals and promotes EMT in endometrial carcinomas, Oncogene 31 (45) (2012) 4778–4788.
[36] A.C. Rodriguez, J.M. Vahrenkamp, K.C. Berrett, et al., ETV4 is necessary for estrogen signaling and growth in endometrial cancer cells, Canc. Res. 80 (6) (2020) 1234–1245.
[37] G. Konings, L. Brentjens, B. Delvoux, et al., Intracrine regulation of estrogen and other sex steroid levels in endometrium and non-gynecological tissues; Pathology, physiology, and drug discovery, Front. Pharmacol. 9 (2018) 940.
[38] T. Heinosalo, N. Saarinen, M. Poutanen, Role of hydroxysteroid (17beta) dehydrogenase type 1 in reproductive tissues and hormone-dependent diseases, Mol. Cell. Endocrinol. 489 (2019) 9–31.
[39] T. Saloniemi, P. Jarvensivu, P. Koskimies, et al., Novel hydroxysteroid (17beta) dehydrogenase 1 inhibitors reverse estrogen-induced endometrial hyperplasia in transgenic mice, Am. J. Pathol. 176 (3) (2010) 1443–1451.
[40] B. Delvoux, T. D'Hooghe, C. Kyama, et al., Inhibition of type 1 17beta-hydroxysteroid dehydrogenase impairs the synthesis of 17beta-estradiol in endometriosis lesions, J. Clin. Endocrinol. Metab. 99 (1) (2014) 276–284.
[41] F. Li, Z. Zhu, M. Xue, et al., siRNA-based breast cancer therapy by suppressing 17beta-hydroxysteroid dehydrogenase type 1 in an optimized xenograft cell and molecular biology model in vivo, Drug Des. Dev. Ther. 13 (2019) 757–766.
[42] K.J. Jerzak, L. Duska, H.J. MacKay, Endocrine therapy in endometrial cancer: an old dog with new tricks, Gynecol. Oncol. 153 (1) (2019) 175–183.

[43] W.J. van Weelden, L. Massuger, Enitec, J.M.A. Pijnenborg, A. Romano, Anti-estrogen treatment in endometrial cancer: a systematic review, Front Oncol 9 (2019) 359.

[44] K. Lindemann, S. Malander, R.D. Christensen, et al., Examestane in advanced or recurrent endometrial carcinoma: a prospective phase II study by the Nordic Society of Gynecologic Oncology (NSGO), BMC Canc. 14 (2014) 68.

[45] V.W. Setiawan, H.P. Yang, M.C. Pike, et al., Type I and II endometrial cancers: have they different risk factors? J. Clin. Oncol. 31 (20) (2013) 2607–2618.

[46] S. Kommoss, M.K. McConechy, F. Kommoss, et al., Final validation of the ProMisE molecular classifier for endometrial carcinoma in a large population-based case series, Ann. Oncol. 29 (5) (2018) 1180–1188.

[47] L. Paleari, M. Rutigliani, G. Siri, N. Provinciali, N. Colombo, A. Decensi, Aromatase inhibitors as adjuvant treatment for ER/PgR positive stage I endometrial carcinoma: a retrospective cohort study, Int. J. Mol. Sci. 21 (6) (2020).

[48] L. Mileshkin, R. Edmondson, R.L. O'Connell, et al., Phase 2 study of anastrozole in recurrent estrogen (ER)/progesterone (PR) positive endometrial cancer: the PARAGON trial - ANZGOG 0903, Gynecol. Oncol. 154 (1) (2019) 29–37.

[49] B.M. Slomovitz, Y. Jiang, M.S. Yates, et al., Phase II study of everolimus and letrozole in patients with recurrent endometrial carcinoma, J. Clin. Oncol. 33 (8) (2015) 930–936.